Proceedings of the Estonian Academy of Sciences,
2024, **73**, 4, 345–355
https://doi.org/10.3176/proc.2024.4.03
Available online at www.eap.ee/proceedings

Novel droop control strategy for indirect battery management in DC nanogrids

Indrek Roasto*, Andrei Blinov and Dmitri Vinnikov

Department of Electrical Power Engineering and Mechatronics, Tallinn University of Technology, Ehitajate tee 5, 19086 Tallinn, Estonia

Received 4 March 2024, accepted 19 April 2024, available online 24 October 2024

Abstract. This paper proposes a novel droop control strategy for indirect battery management in DC nanogrids. Droop control as a decentralized control method is a well-recognized method to provide effective power sharing and voltage stability among sources and loads in the DC nanogrid without additional communication links. While most existing droop control methods focus on adjusting each individual battery droop curve directly, the proposed method manipulates the droop curve of the active front-end converter, which connects the nanogrid to the main grid to indirectly influence the state of charge of the battery. The method employs a piecewise linear droop curve with a movable inflection point, which can be adjusted according to different scenarios. The effectiveness of the proposed method is evaluated through simulations using real data from a residential house with rooftop PV panels. The results show that the proposed method not only improves battery utilization but also increases renewable energy self-consumption.

Keywords: DC droop control, piecewise linear droop control, DC nanogrid, residential applications, battery management.

1. INTRODUCTION

The ubiquitous requirement for DC voltage in contemporary household appliances has been extensively documented and analysed [1,2]. Among these appliances are some, which by default are supplied from frequency converters, as seen in washing machines, vacuum cleaners, heat pumps, and similar devices. Although supplied by AC, they are also fully compatible with DC voltage. Moreover, by using DC instead of AC voltage, higher efficiencies could be achieved [3]. Consequently, there has been a discernible trend towards DC distribution, particularly within residential structures.

A compelling rationale for the adoption of DC power in residential buildings is the proliferation of renewable energy sources and storage systems inherently operating at DC voltages. In the contemporary energy landscape, residential buildings are no longer mere energy consumers but rather active participants within microgrids. Through integration with local renewable energy sources and storage infrastructure, households effectively function as small-scale microgrids or nanogrids capable of fulfilling their energy demands autonomously while potentially contributing surplus energy to the main grid. Effective operation of such nanogrids necessitates specialized control strategies to ensure efficiency and sustainability [4].

While centralized control from a master device offers a conceptually appealing approach to nanogrid management, practical implementation could be challenging due to high-speed communication requirements. Considering the dynamic nature of power electronics-based nanogrids, characterized by diverse transient timescales, designing a suitable communication interface presents technical hurdles and economic feasibility concerns. Consequently, decentralized control methods devoid of explicit communication links emerge as preferable options [5].

Droop control, a decentralized control technique well-established in AC systems for achieving stable and equitable load sharing among parallel sources and loads without additional communication links, proves beneficial

* Corresponding author, indrek.roasto@ieee.org

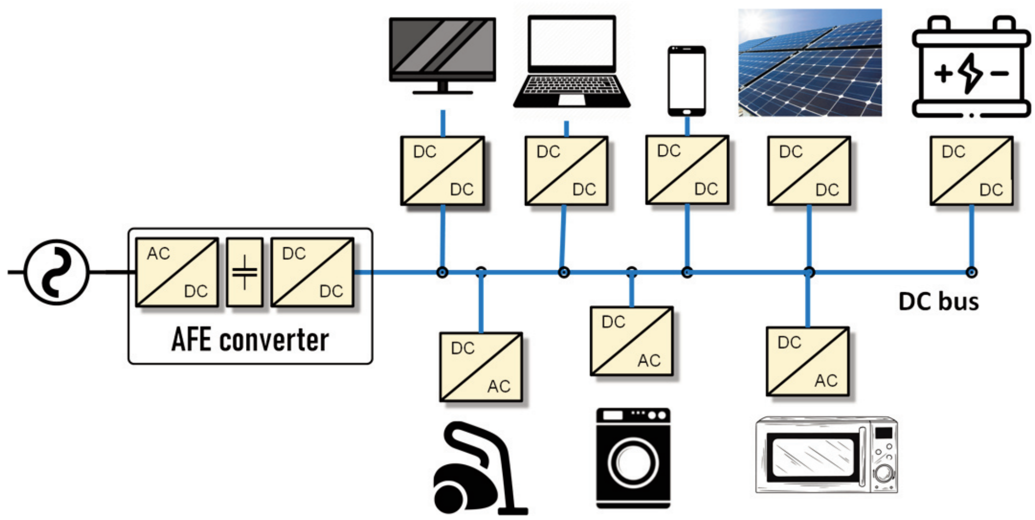

Fig. 1. A vision of the residential DC nanogrid.

also for DC systems. Particularly suited to power electronics-dominated grids where all sources and loads are interfaced with the grid via power electronics, droop control presents an attractive solution for effective energy management and power sharing.

In [4], an extensive description of a future residential building's structure based on DC droop control is provided. The concept involves connecting storage, sources, and loads via a common DC bus, thus eliminating AC voltage within the building, as shown in Fig. 1. Additionally, the building will link to the AC grid at the point of common coupling through a bidirectional power electronic converter, also referred to as the active front-end (AFE). For enabling island mode operation, the residential building must incorporate local generation and energy storage (ES). Through droop control, various objectives, such as enhancing power sharing, compensating line resistances, ES management, etc., can be accomplished. The main goal of this paper is to analyse different droop control aspects from the storage utilization perspective.

Numerous papers discuss various ES management strategies in the DC nanogrid using droop control. A prevalent approach is to employ fixed droop coefficients for each node (load, ES, or renewable energy source) and utilize DC bus signalling for scheduling generation from different sources [6]. Modification of ES charging and discharging rates can be achieved by shifting droop curves. As a drawback, this often necessitates an additional low-speed communication channel [6]. More sophisticated methods are necessary for managing multiple ES units. In [7,8], adaptive droop control was utilized to balance the state of charge (SoC) of multiple ES units in the DC nanogrid. Droop coefficients of ES units were made inversely proportional to the SoC, leading to quicker discharge when the SoC was high and slower discharge when the SoC was low. Over time, this resulted in balanced SoC across all ES units, thereby achieving equal power sharing. Further advancements in adaptive droop control were explored in [9], introducing different SoC-dependent droop coefficients for charging and discharging and incorporating dead zones into the droop curves to prevent simultaneous charging and discharging of different ES units. Similar concepts with slight variations were discussed in [5]. Additionally, droop coefficients can be modified to be either more resistive or inductive depending on the ES type [10]. A resistive droop coefficient was applied on a super capacitor to compensate for fast power transients, while an inductive droop coefficient was implemented to deliver average load power with the battery.

Droop control offers diverse strategies for regulating power flow and managing ES within the DC nanogrid. However, existing research primarily concentrates on adjusting ES droop curves to optimize energy storage management. This paper introduces a new perspective: altering the droop curve of the AFE converter indirectly influences the SoC of ES without necessitating direct communication. To achieve this, a piecewise linear droop curve is employed. By adjusting the inflection point of the droop curve upward or downward, the SoC of ES can be manipulated. Furthermore, simulations demonstrate that this adjustment also impacts renewables self-consumption (RSC).

The paper is structured into five chapters: the introduction is followed by an overview of droop control principles, DC bus signalling, and different methods for manipulating droop curves. In the third chapter, the proposed concept is clarified and compared with conventional droop control principles. In the fourth chapter, the proposed method is validated through computer simulations based on a real dataset. Specifically, the PV generation and consumption profiles utilized in the simulations were collected through logging at an actual household in Estonia. Unlike many other studies where simulation durations tend to be relatively short (ranging from seconds to hours), this research extends over a one-week timeframe, which the authors believe offers an optimal duration for evaluating the effects of any droop control strategy.

2. PRINCIPLES OF DROOP CONTROL AND DC BUS SIGNALLING

In DC microgrids, maintaining stable voltage and ensuring proportional power sharing among connected devices are crucial aspects for reliable operation. However, conventional voltage-mode converters lack direct control over their output power. This creates a challenge when connecting them in parallel to a DC grid. With multiple voltage sources competing, unequal power distribution can lead to circulating currents and potential voltage instability [11].

DC droop control provides a decentralized and elegant solution for regulating power sharing in DC microgrids. Sources operate in current mode control, which inherently avoids circulating currents. Each source introduces a 'virtual resistance', also known as the droop coefficient, that automatically adjusts its output voltage based on the injected current according to the following equation:

$$u_o^*(t) = u_{dc} - i_o(t) \cdot r_d \,, \quad (1)$$

where u_o^* is the output voltage reference, u_{dc} is the output voltage in no load condition (constant), i_o is the measured output current, and r_d is the droop coefficient. Through the introduction of a virtual resistance, the reference voltage at each source's output inversely tracks the increase in the output current. This inherently limits the output power, allowing adjustment through the choice of droop coefficients. The droop coefficient must be calculated for each distributed energy source (DES) separately. Droop coefficients can be calculated as follows [12]:

$$r_d \le \frac{\Delta u_{dc}}{i_{o\_max}} \,, \quad (2)$$

where Δu_{dc} is the maximum allowed DC bus voltage variation range (typically ±10%) and i_{o_max} is the maximum output current of the corresponding DES.

By rearranging (1), the output current reference can be directly calculated as:

$$i_o^*(t) = \frac{u_{dc} - u_o(t)}{r_d}, \quad (3)$$

where $u_o(t)$ is the measured output voltage. This method, also known as *I-U* droop control, is simpler and has faster dynamics than the typical *U-I* droop control [13]. This method was also used in the current research.

While DC droop control effectively facilitates power sharing in microgrids, its inability to differentiate between diverse DES remains a limitation. This challenge is addressed by the superimposed DC bus signalling method, facilitating information exchange among DES, storage, and loads without dedicated communication channels. Moreover, the DC bus voltage itself acts as the information carrier. This method conceptually relies on segmenting the droop voltage range into distinct priority zones, as shown in Fig. 2. Within each priority zone, only the designated converter group actively regulates the bus voltage through droop control. This zonation allows limited DC bus voltage fluctuations within defined boundaries, typically around ±10%, as reported in studies [14,15]. For deviations exceeding these limits, overvoltage or undervoltage protection mechanisms are triggered.

2.1. Modifying the slope of the droop curves

Equation (1) can be interpreted as a linear relationship, where the droop coefficient acts as the gradient and u_{dc} represents the voltage axis intercept of the *U-I* curve. However, (2) solely establishes the maximum achievable r_d value without restricting lower values. This flexibility can be realized by manipulating the Δu_{dc} parameter. Modifying the r_d value alters the slope of the *U-I* curve, as shown in Fig. 3. Within the context of a DC nanogrid, this implies that the corresponding source can be tailored to offer stronger bus voltage support. In general, the shallower the slope, the faster response from the converter power output can be expected.

Within ES systems, the droop coefficient possesses the potential to be dynamically linked to the SoC, offering a mechanism to prevent overcharging and overdischarging [16]. Furthermore, implementing different coefficients for charging and discharging (Fig. 4) enables a more aggressive discharging profile compared to charging, often recommended by battery manufacturers due to inherent electrochemical limitations. The droop curve with two or more slopes, also known as piecewise linear droop, was implemented in this research for the AFE control.

2.2. Shifting the droop curves

The *U-I* droop curves have the capability to be shifted along the voltage axis, as illustrated in Fig. 5. Adjusting the droop curves upwards or downwards enables the positioning of the converter within various priority zones regarding DC bus signalling and alters the point at which energy flow reverses. For instance, lowering the droop

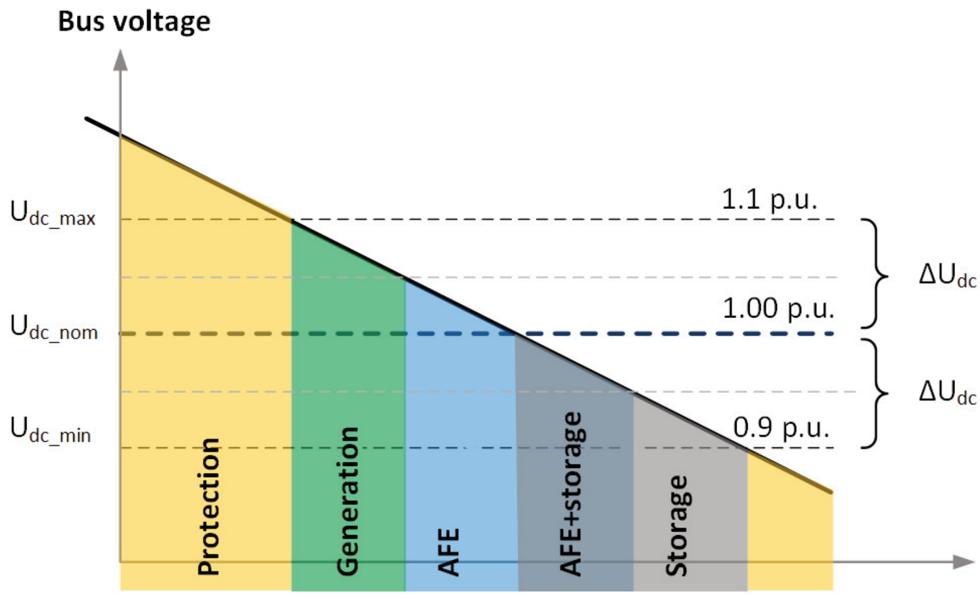

Fig. 2. DC bus signalling utilizes bus voltage for communication.

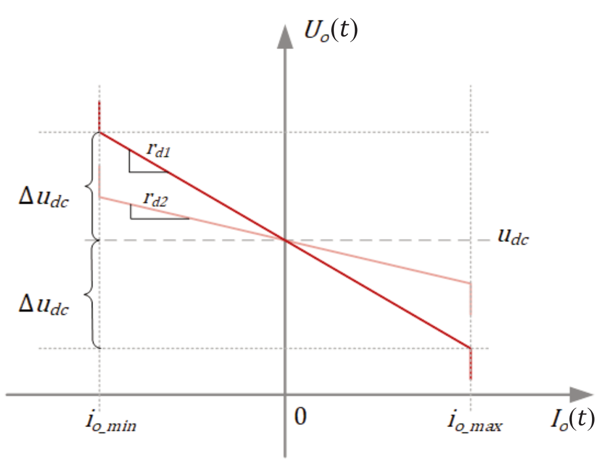

Fig. 3. *U-I* droop curves with different droop coefficients.

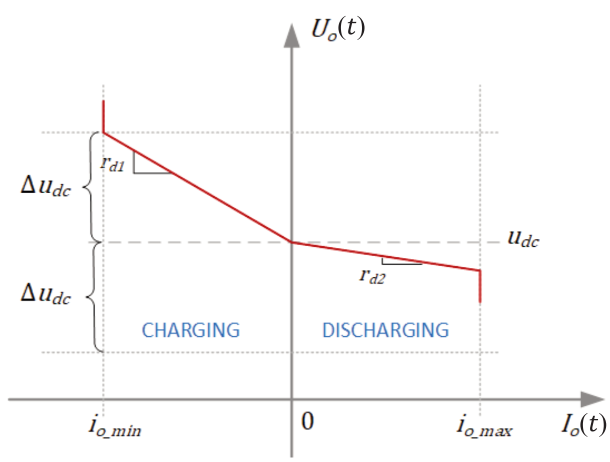

Fig. 4. Different droop coefficients for charging and discharging.

curve by 5% (as depicted by the blue line in Fig. 5) shifts the dominance region of the converter downwards. Consequently, it maintains regulation of the grid voltage at lower levels and achieves the i_{o_min} threshold earlier. Once i_{o_min} is attained, the converter transitions into the constant current mode control, ceasing regulation of the bus voltage. Energy flow reversal occurs when the bus voltage value drops 5%. However, there is a drawback: the maximum output current i_{o_max} can never be reached as it falls below the minimum allowable bus voltage level, as shown in Fig. 5. This issue could be remedied by reducing the slope of the *U-I* curve. The same principle applies when elevating the droop curves; the converter then regulates the bus voltage at higher values, relinquishing dominance at lower values.

2.3. Changing the shape of the droop curves

The droop curves can exhibit various forms, including linear, piecewise linear, or nonlinear [17]. In a piecewise linear droop curve, the droop voltage range is divided into multiple linear segments, while nonlinear droop curves take on polynomial shapes. Typically, the motivation for altering droop curves stems from the desire to compensate for line impedances, enhance voltage regulation, or improve power sharing. Polynomial-shaped droop curves are

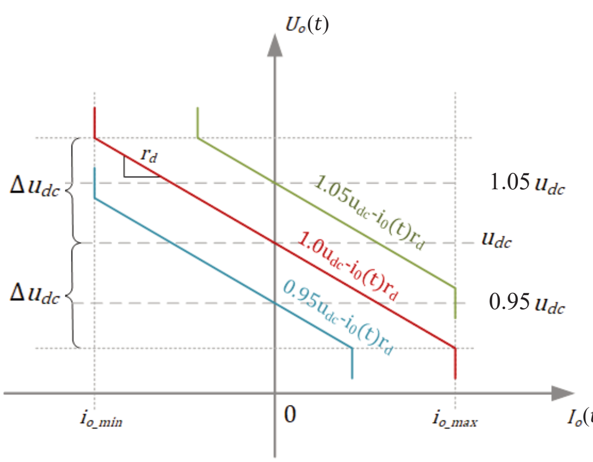

Fig. 5. Droop curves can be shifted along the voltage axis.

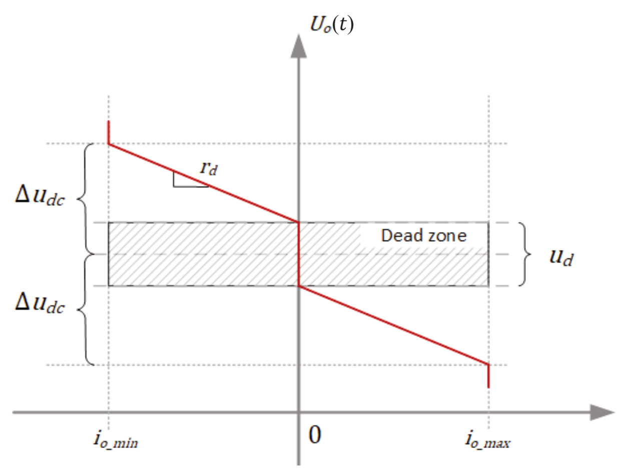

Fig. 6. Linear droop curve with added dead zone.

particularly useful for compensating for line impedances. Generally, as line impedance increases, so does the deviation in load sharing when the droop coefficient remains fixed. By making the droop coefficient dependent on the load current, more precise power sharing and voltage control can be achieved [17].

To enhance the energy management of ES, employing piecewise linear droop control with a dead zone could prove beneficial. This entails splitting a linear droop curve into two segments by introducing a dead zone in the no-load area, as shown in Fig. 6.

Within the dead zone, the associated converter operates in standby mode. Standby mode means no power delivery. The overarching concept is to inhibit particular DES or ES units and enable other sources to predominate within that designated voltage range. This approach has proven effective in preventing simultaneous charging and discharging of multiple ES units [18]. The magnitude of the dead zone can be adjusted according to requirements. The droop coefficient can be determined using the following formula:

$$r_d \leq \frac{\Delta u_{dc} - 0.5 \cdot u_d}{i_{o\_max}}, \tag{4}$$

where u_d is the dead zone range measured in volts.

3. CONVENTIONAL VS PROPOSED PIECEWISE LINEAR DROOP CONTROL

The nanogrid in the current case consisted of rooftop PV panels, household loads, a battery, and AFE. The operation of each device directly depends on the DC bus voltage. The voltage is allowed to deviate from the nominal bus voltage by up to 10% on either side (Fig. 7). A voltage rise indicates an excess of energy, while a voltage drop

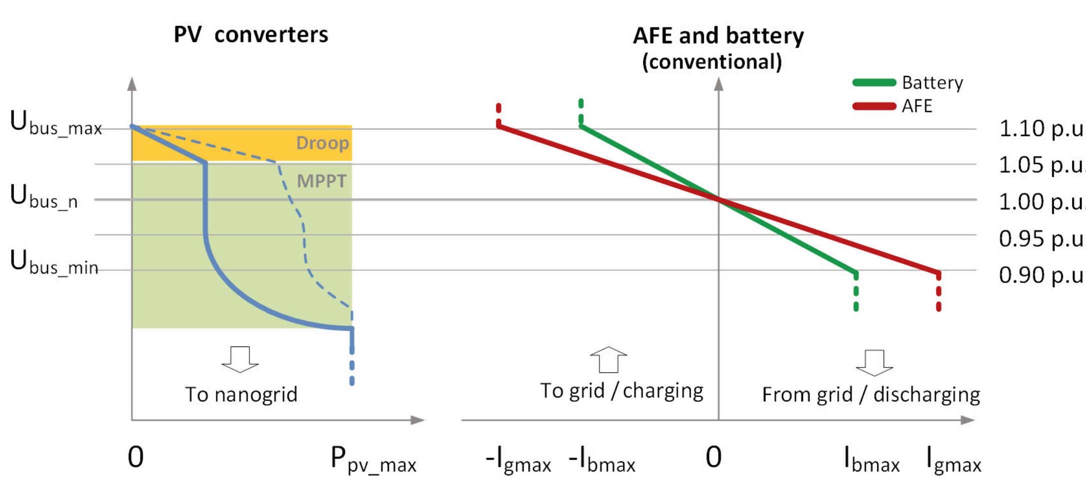

Fig. 7. Conventional droop control for residential nanogrid.

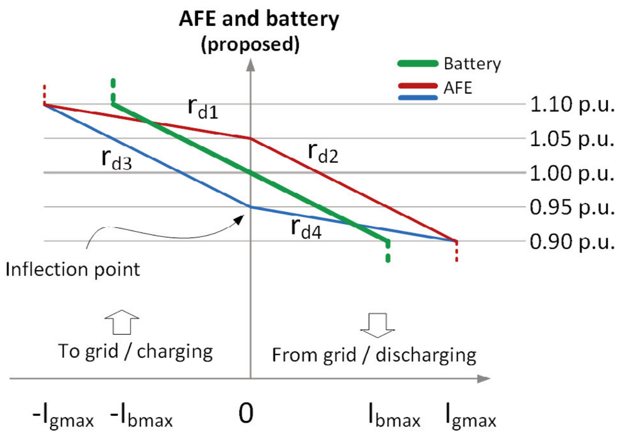

Fig. 8. Proposed piecewise linear droop control for residential nanogrid.

indicates a lack of energy in the nanogrid. PV panels typically operate in MPPT mode, except when the bus voltage exceeds the 1.05 per unit (p.u.) voltage level. This level indicates an excess of power, and the PV converter will switch into droop control mode, as shown in Fig. 7.

In the case of conventional droop control, the battery and AFE droop curves are both linear and centred at the nominal bus voltage value (currently 350 V), as shown in Fig. 7. The droop coefficients can be computed according to (2). Centred droop curves provide proportional power sharing between the AFE and the battery converter. In general, grid/battery mode refers to a negative droop current, i.e. the energy is injected to the mains or to the battery. Nanogrid mode refers to a positive droop current, i.e. the energy taken from the mains or the battery is moving to the nanogrid.

The proposed piecewise linear droop curve allows defining different droop slopes for the grid and nanogrid mode of the AFE, as depicted in Fig. 8. The point where these lines intersect on the voltage axis is termed the inflection point. Theoretically, shifting this point upward along the voltage axis (as indicated by the red curve in Fig. 8) results in the AFE supplying more energy to the nanogrid. In scenarios where the load remains unchanged, this surplus energy will be charged into batteries. Conversely, by adjusting the inflection point below the nominal bus voltage (as shown by the blue curve in Fig. 8), the AFE will begin injecting more energy into the main grid, thereby increasing the discharge rate of batteries.

It is possible to change the droop curves during operation dynamically. This capability enables the utilization of various droop curve patterns tailored to different circumstances. For instance, one could adjust the inflection point based on factors such as electricity prices, PV generation, and other relevant variables.

4. SIMULATION RESULTS AND ANALYSIS

The effectiveness of the proposed droop control strategy was evaluated through numerical simulations in PLECS software. The model encompassed a simplified single-phase microgrid consisting of a PV converter with MPPT, a battery storage unit, the AFE converter, and a representative load, as depicted in Fig. 9. The AFE, located at the point of common coupling, managed energy flow between the grid and the residential house.

To prioritize the investigation of control strategy performance rather than the intricate dynamics of individual power electronics components, the model adopted a simplified approach. All power electronics converters were modelled as ideal, programmable current sources (Fig. 9), and the load was represented as a variable resistor. This simplification facilitated faster simulations and longer simulation timeframes. The specific parameters employed in the simulation are detailed in Table 1.

For enhanced realism, the simulations incorporated actual PV generation and load consumption profiles harvested from a single-family home in Estonia equipped with rooftop PV panels and an electric vehicle. The house, situated in a village near Tallinn, utilized a heat pump, kitchen appliances, a ventilation unit, and an electric sauna as primary electricity consumers. Additionally, a BMW i3 electric vehicle was routinely charged overnight. Data logging was performed using a Linax PQ1000 two-channel industrial logger, recording both PV generation and load consumption with a 10-second time resolution. Specifically, logger data from April 2023 was employed for this study, representing a one-week timeframe (seven days). The data was imported from a CSV file into PLECS and scaled to achieve a simulation time of 60.48 seconds, corresponding to one week in realtime.

In Fig. 10, the measured load and consumption profiles of the house during the simulation period are de-

Table 1. Simulation parameters

Parameter	Value
PV maximum power	4 kW
Nominal DC-link voltage	350 V
Battery storage	
Nominal capacity	13 kWh
Usable capacity	12 kWh
Continuous power	5 kW
Initial SoC	100%
AFE	
Power	15 kW
Maximum DC current	43 A

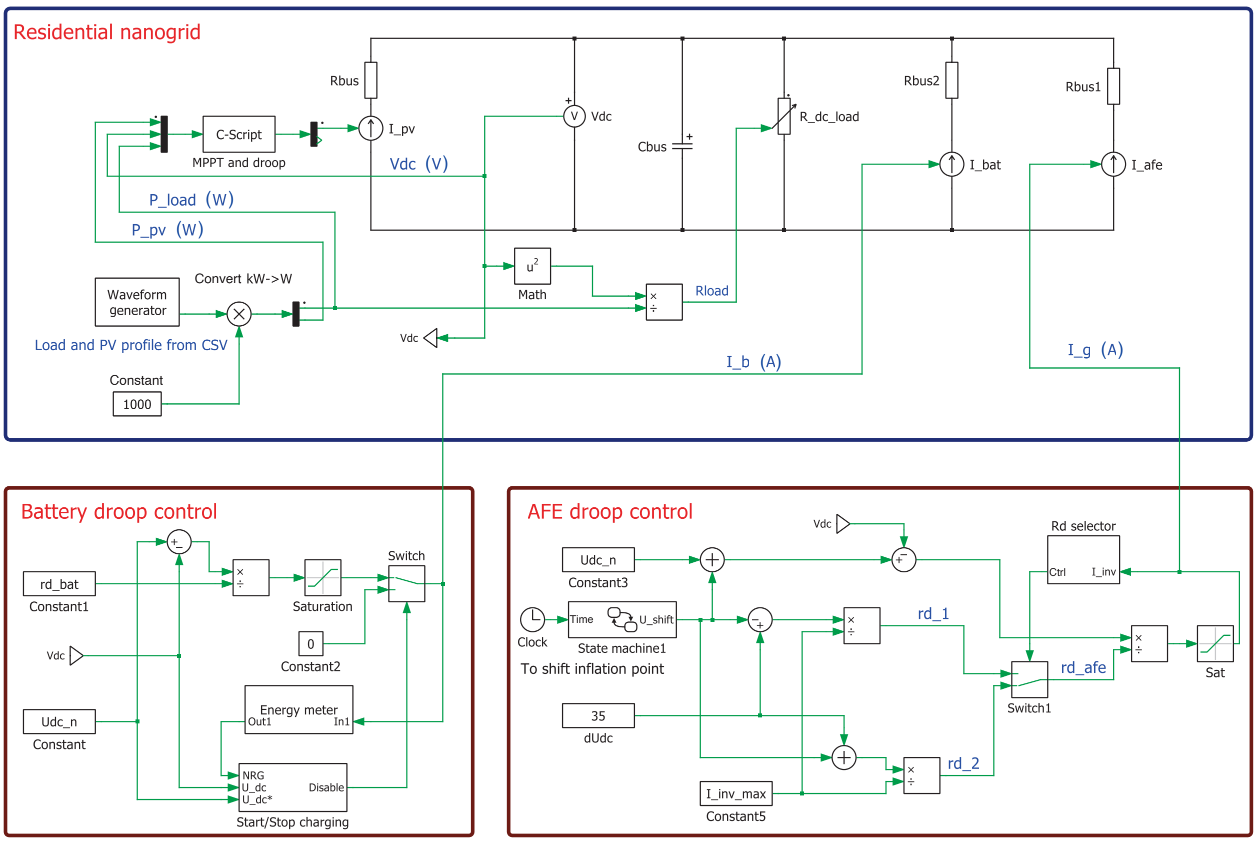

Fig. 9. PLECS model of the DC nanogrid with the droop control.

picted. PV generation exhibited relative stability for five days, reaching a peak production of 4 kW. Cloud cover significantly impacted generation, reducing peak power to 800 W on the fifth day and causing fluctuations between 1 and 4 kW on the sixth day. The load fluctuated between 120 W and 10.2 kW, reflecting diverse household activities. The average daily consumption remained around 2.5 kW throughout the simulated week.

This study aimed to compare and evaluate the influence of conventional linear droop control and piecewise linear droop control on battery storage within a DC nanogrid. The fundamental hypothesis was that manipulating the inflection point of the AFE droop curve could indirectly regulate battery SoC without requiring direct communication between the AFE and the battery storage.

To ensure realism, the investigation utilized actual load and PV generation profiles recorded from a single-family house. However, given the absence of bidirectional battery storage in the actual household – a crucial component for DC nanogrids – a virtual battery was incorporated within the PLECS simulation environment. The real-world electric vehicle present in the house was modelled as a unidirectional load due to its limited functionality.

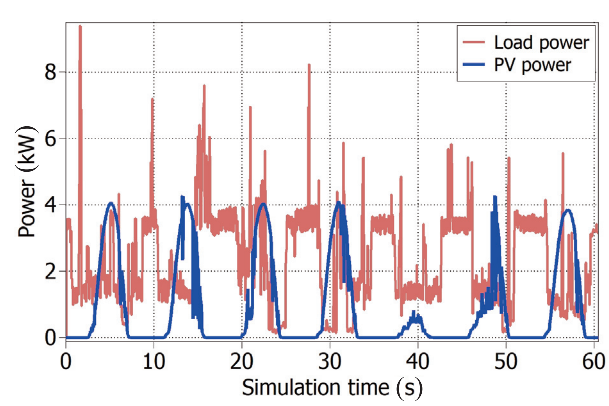

Fig. 10. PV and load power profiles over one week. Time scale: 8 s ~ 1 day.

The virtual battery parameters were derived from a commercially available Tesla Powerwall 2 DC model, characterized by a usable energy capacity of 13.5 kWh. All simulations commenced with the battery fully charged (SoC = 100%). Additionally, a nominal DC bus voltage of 350 V was adopted, aligning with the Netherlands DC low voltage standard NPR 9090 [19].

4.1. Implemented metrics

Typically, it is advisable to maximize the utilization of renewable energy resources directly at the location of the generation. This is called renewables self-consumption (RSC). The RSC in the current research was calculated as

$$RSC = \frac{E_{PV} - E_{grid}}{E_{PV}}, \tag{5}$$

where E_{PV} is the energy produced by PV panels and E_{grid} is the energy injected to the grid. However, practical implementation of the RSC proves challenging due to the inherent mismatch between production and consumption patterns. This challenge can be addressed by employing ES with appropriate control mechanisms. ES makes it possible to store renewable energy locally and use it later when there is a need for it. As one of the aims of this study was to assess the impact of piecewise linear droop curves on the RSC, it served as the primary metric in subsequent simulations.

Before improving RSC, it is essential to ascertain the baseline value, i.e. RSC without droop control and ES. This baseline value is specific to each case and requires individual measurement for accurate determination. In the current study case, was calculated to be 55%, which refers to a relatively good match between the load and PV production.

Another goal of the current research was to demonstrate how SoC of the battery can be influenced by the AFE without any communication. This was achieved by employing a piecewise linear droop curve with the movable inflection point in the AFE. To estimate the effectiveness of this proposed method, average SoC over the full simulation period (one week in real time) was measured.

4.2. Simulation of the conventional droop control

Conventional droop control provides an effective method for power sharing between sources, but it is less efficient for storage management. The simulation (Fig. 11) shows that the battery was never charged more than 25% and was fully discharged most of the time. On the fifth day (a cloudy day), the batteries were not charged at all. The average SoC over a week's time was only 14%, indicating suboptimal battery utilization. However, RSC with centred droop curves reached 73%, which is a considerable improvement compared to RSC without the droop control.

4.3. Simulation of the piecewise linear droop control

The utilization of a piecewise linear droop curve offers a means to influence the SoC of a battery without direct communication. This effect was examined through two simulations, where the inflection point (cross-over voltage) was set at 346 V and 358 V, as depicted in Fig. 12. All other parameters of the model, including the load profile, PV production, and the battery droop curve, remained constant. Notably, adjusting the inflection point produced a substantial impact on the battery's SoC. Specifically, lowering the inflection point below the nominal bus voltage prompted the AFE to inject more energy into the main grid, thereby preventing the battery bank from reaching full charge. Consequently, the average

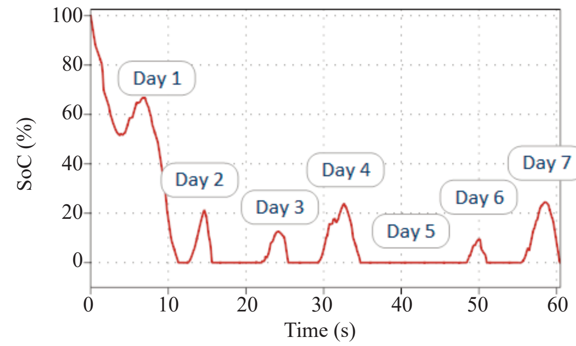

Fig. 11. SoC in the case of centred droop curves.

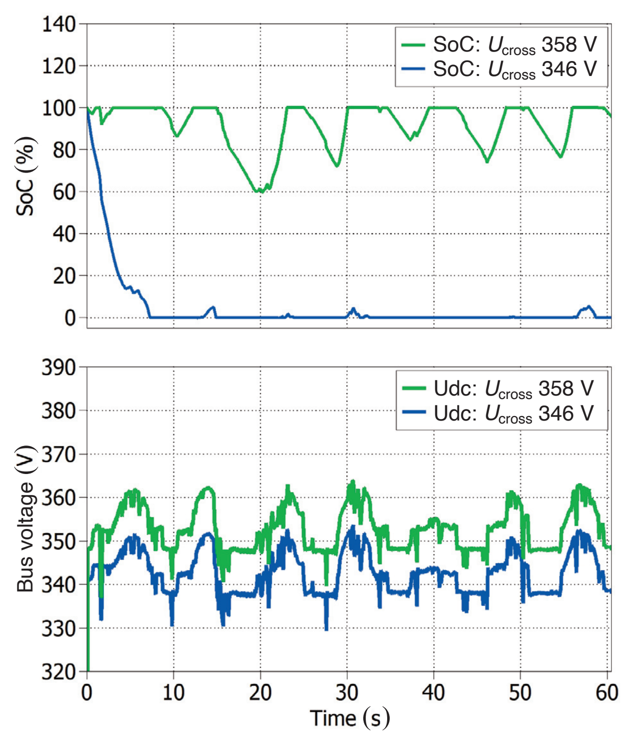

Fig. 12. By moving the inflection point of the AFE droop curve (from 346 V to 358 V), SoC and DC bus voltage change. Time scale: 8 s ~ 1 day.

SoC of the battery bank hovered around 4%, indicating a strong underutilization of the battery bank. Furthermore, the RSC attained only 63%, representing a 10% reduction compared to conventional centrally positioned droop curves. This observation implies that PV energy was predominantly channelled into the grid rather than stored locally. Such a strategy could prove advantageous in market-driven nanogrid control scenarios, where maximizing energy injection into the grid is prioritized during periods of high pricing.

Elevating the inflection point beyond the nominal bus voltage value induces the AFE to prioritize grid energy consumption, thereby leading to a predominantly charged state of the batteries, as shown in Fig. 12. The average SoC of the battery bank was 92%, indicating underuse of the battery. Furthermore, the RSC attained 68%, suggesting that the battery bank primarily relied on PV energy to maintain its charge, while the load was predominantly supplied from the main grid. This approach holds potential utility in reliability-centric applications, where battery backup power is imperative to mitigate power interruptions.

It is pertinent to note that the adjustment of the inflection point of the droop curve did not alter the waveform of the bus voltage but did influence its average value. For instance, setting the crossover voltage at 346 V yielded an average DC bus voltage of 338 V, whereas the crossover voltage of 358 V corresponded to an average DC bus voltage of 348 V. In conclusion, elevating the inflection point prompts the AFE to increase energy delivery from the grid, subsequently raising the bus voltage. Elevated bus voltage leads to reduced battery utilization. Conversely, lowering the inflection point compels the AFE to inject more energy into the grid, resulting in a decreased bus voltage and consequently increased storage utilization.

4.4. Simulation of dynamically changing droop curves

The inflection point of the AFE could also be changed dynamically based on some higher-level control strategy, e.g. intensity of the sun radiation. To store PV energy locally and use it on site, the batteries should be charged during daytime and discharged during night. The AFE can achieve this goal by elevating the inflection point during daytime and lowering it during night. In the following simulation, the inflection point was changed daily as follows (Fig. 13): during the day from 10:00 AM to 08:00 PM, the inflection point was set to U_{cross} = 357 V, and during the night after 08:00 PM, the inflection point was set to U_{cross} = 351 V. To show the effect, the inflection point values were chosen randomly. However, it is expected that even better results could be achieved through optimization. This control strategy resulted in increased battery utilization compared to the conventional static droop control (Fig. 14). The SoC of the battery bank exhibited wider fluctuations, ranging from 0% to 100%, with an average SoC variation of 39%. Furthermore, the RSC increased from 73% to 86%, demonstrating the effectiveness of the AFE in influencing the RSC through dynamic droop curve adjustments.

4.5. Generalizations

The conventional droop control is a well-established technique for achieving power sharing in nanogrids. While it demonstrably achieves a relatively high RSC value (Table 2), further improvements in battery and energy management can be attained through the implementation of dynamically changing piecewise linear droop curves for the AFE converter. This approach has been shown to yield an 18% increase in RSC and a 2.8-fold increase in average battery SoC compared to the conventional method. Piecewise linear droop methods with static curves (methods 2 and 3) achieved intermediate RSC values and exhibited varying effects on average SoC, as detailed in Table 2. These findings suggest that such methods may be suitable for specific applications requir-

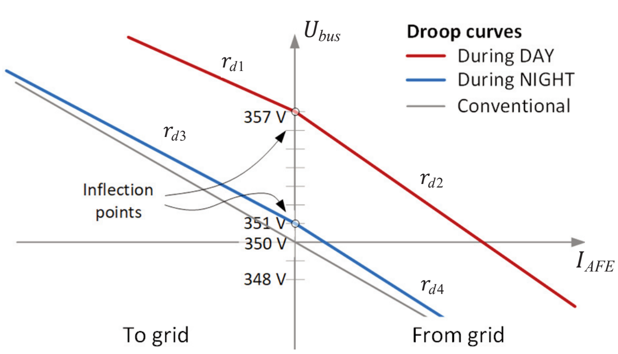

Fig. 13. Dynamically shifting droop curves of the AFE.

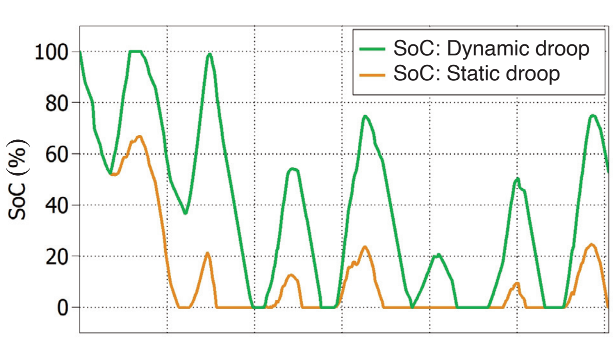

Fig. 14. Dynamic vs static droop control.

Table 2. Comparison of different droop control methods

No.	Algorithm	RSC (%)	Average SoC (%)
1	Conventional droop control	73	14
2	Droop with inflection point above nominal bus voltage	68	92
3	Droop with inflection point below nominal bus voltage	63	4
4	Dynamically changing droop curve	86	39

ing particular trade-offs between stability and energy management, as previously discussed.

5. CONCLUSIONS

Droop control is prevalent in DC microgrids, where distributed sources regulate DC bus voltage through individual droop curves. Existing literature primarily focuses on modifying battery droop curves for optimized energy storage management. This paper presents a novel perspective: manipulating the droop curve of the AFE converter influences the SoC of batteries without direct communication. Piecewise linear droop curves were analysed regarding inflection point shift with the following results:

- Upward shift results in the AFE supplying more energy to the nanogrid and thus forcing batteries to charge.
- Downward shift results in the AFE injecting more energy to the main grid, thereby increasing the discharge rate of batteries.

The proposed droop control strategy's efficacy was evaluated through simulations replicating real-world operating conditions. PV generation and load profiles gathered from an existing household served as simulation inputs. These simulations revealed that conventional droop control methodologies cannot achieve optimal battery utilization, as evidenced by an average SoC of only 14% for the battery bank over a week and a renewables self-consumption of 73% obtained with centred droop curves.

Piecewise linear droop curves demonstrate potential for improved battery utilization. However, over-optimization poses risks: excessively shifting the inflection point can isolate batteries by keeping them perpetually charged or discharged, hindering their functionality. This highlights the importance of finding the optimal balance.

The most promising results were achieved using dynamically changing piecewise linear droop curves for the AFE converter. This approach yielded an 18% increase in RSC and a 2.8-fold increase in average battery SoC compared to the conventional method.

Dynamically changing piecewise linear droop curves offer a simpler and potentially more robust alternative to conventional battery droop curve modifications, warranting further investigation and potential applications in practical microgrid scenarios.

ACKNOWLEDGEMENTS

This research was supported by the Estonian Research Council under grant PRG1086 and in part by the Estonian Centre of Excellence in Energy Efficiency (ENER), grant TK230, funded by the Estonian Ministry of Education and Research. The publication costs of this article were covered by the Estonian Academy of Sciences.

REFERENCES

1. Lee, P.-W., Lee, Y.-S. and Lin, B.-T. Power distribution systems for future homes. In *Proceedings of the IEEE 1999 International Conference on Power Electronics and Drive Systems (PEDS'99), Hong Kong, China, 27–29 July 1999*. IEEE, 1999, **2**, 1140–1146. https://doi.org/10.1109/peds.1999.792869
2. Ganesan, S. I., Pattabiraman, D., Govindarajan, R. K., Rajan, M. and Nagamani, C. Control scheme for a bidirectional converter in a self-sustaining low-voltage DC nanogrid. *IEEE Trans. Ind. Electron.*, 2015, **62**(10), 6317–6326. https://doi.org/10.1109/TIE.2015.2424192
3. Gerber, D. L., Vossos, V., Feng, W., Marnay, C., Nordman, B. and Brown, R. A simulation-based efficiency comparison of AC and DC power distribution networks in commercial buildings. *Appl. Energy*, 2018, **210**, 1167–1187. https://doi.org/10.1016/j.apenergy.2017.05.179
4. Boroyevich, D., Cvetković, I., Dong, D., Burgos, R., Wang, F. and Lee, F. Future electronic power distribution systems a contemplative view. In *12th International Conference on Optimization of Electrical and Electronic Equipment, Brasov, Romania, 20–22 May 2010*. IEEE, 2010, 1369–1380. https://doi.org/10.1109/OPTIM.2010.5510477
5. Nguyen, T. L., Guerrero, J. M. and Griepentrog, G. A self-sustained and flexible control strategy for islanded DC nanogrids without communication links. *IEEE J. Emerg. Sel. Topics Power Electron.*, 2020, **8**(1), 877–892. https://doi.org/10.1109/JESTPE.2019.2894564
6. Zhang, W., Lee, F. C. and Huang, P.-Y. Energy management system control and experiment for future home. In *IEEE Energy Conversion Congress and Exposition (ECCE), Pittsburgh, PA, USA, 14–18 September 2014*. IEEE, 2014, 3317–3324. https://doi.org/10.1109/ECCE.2014.6953851

7. Lu, X., Sun, K., Guerrero, J. M., Vasquez, J. C. and Huang, L. State-of-charge balance using adaptive droop control for distributed energy storage systems in DC microgrid applications. *IEEE Trans. Ind. Electron.*, 2014, **61**(6), 2804–2815. https://doi.org/10.1109/TIE.2013.2279374
8. Su, J., Li, K., Li, Y., Xing, C. and Yu, J. A novel state-of-charge-based droop control for battery energy storage systems to support coordinated operation of DC microgrids. *IEEE J. Emerg. Sel. Topics Power Electron.*, 2023, **11**(1), 312–324. https://doi.org/10.1109/JESTPE.2022.3149398
9. Narayan, N., Mackay, L., Malik, B. O., Popovic-Gerber, J., Qin, Z., Bauer, P. et al. Decentralized control-scheme for DC-interconnected solar home systems for rural electrification. In *IEEE 3rd International Conference on DC Microgrids (ICDCM), Matsue, Japan, 20–23 May 2019*. IEEE, 2019, 1–6. https://doi.org/10.1109/ICDCM45535.2019.9232831
10. Song, Q. and Chen, J. A decentralized energy management strategy for a battery/supercapacitor hybrid energy storage system in autonomous DC microgrid. In *IEEE 27th International Symposium on Industrial Electronics (ISIE), Cairns, QLD, Australia, 13–15 June 2018*. IEEE, 19–24. https://doi.org/10.1109/ISIE.2018.8433728
11. Ito, Y., Zhongqing, Y. and Akagi, H. DC microgrid based distribution power generation system. In *The 4th International Power Electronics and Motion Control Conference (IPMC), Xi'an, China, 14–16 August 2004*. IEEE, 2004, 2352–2360.
12. Hailu, T., Mackay, L., Ramirez-Elizondo, L., Gu, J. and Ferreira, J. A. Voltage weak DC microgrid. In *IEEE First International Conference on DC Microgrids (ICDCM), Atlanta, GA, USA, 7–10 June 2015.* IEEE, 2015, 138–143.
13. Lu, X., Guerrero, J. M., Sun, K. and Vasquez, J. C. An improved droop control method for DC microgrids based on low bandwidth communication with DC bus voltage restoration and enhanced current sharing accuracy. *IEEE Trans. Power Electron.*, 2014, **29**(4), 1800–1812. https://doi.org/10.1109/TPEL.2013.2266419
14. Zeng, W., Sun, M., Chen, B., He, W., Xiong, H. and Xiong, J. Stability analysis of energy routing system considering droop control. In *IEEE 3rd Conference on Energy Internet and Energy System Integration (EI2), Changsha, China, 8–10 November 2019*. IEEE, 2019, 1024–1029. https://doi.org/10.1109/EI247390.2019.9062170
15. Liu, G., Mattavelli, P. and Saggini, S. Design of droop controllers for converters in DC microgrids towards reducing bus capacitance acknowledgments. In *20th European Conference on Power Electronics and Applications (EPE'18 ECCE Europe), Riga, Latvia, 17–21 September 2018.* IEEE, 2018, P1–P9.
16. Su, J., Li, K., Li, Y., Xing, C. and Yu, J. A novel state-of-charge-based droop control for battery energy storage systems to support coordinated operation of DC microgrids. *IEEE J. Emerg. Sel. Topics Power Electron.*, 2023, **11**(1), 312–324. https://doi.org/10.1109/JESTPE.2022.3149398
17. Chen, F., Burgos, R., Boroyevich, D., Vasquez, J. C. and Guerrero, J. M. Investigation of nonlinear droop control in DC power distribution systems: load sharing, voltage regulation, efficiency, and stability. *IEEE Trans. Power Electron.*, 2019, **34**(10), 9407–9421. https://doi.org/10.1109/TPEL.2019.2893686
18. Narayan, N., Mackay, L., Malik, B. O., Popovic-Gerber, J., Qin, Z., Bauer, P. et al. Decentralized control-scheme for DC-interconnected solar home systems for rural electrification. In *IEEE Third International Conference on DC Microgrids (ICDCM)*, *Matsue, Japan, 20–23 May 2019*. IEEE, 2019, 1–6. https://doi.org/10.1109/ICDCM45535.2019.9232831
19. Royal Dutch Standardization Institute (NEN). *NL: DC Installations for Low Voltage, Standard NPR 9090:2018*.

Uudne *droop*-juhtimismeetod aku kaudseks haldamiseks alalisvoolu nanovõrgus

Indrek Roasto, Andrei Blinov ja Dmitri Vinnikov

Artiklis pakutakse välja uudne *droop*-juhtimisstrateegia aku kaudseks haldamiseks alalisvoolu nanovõrkudes. *Droop*-juhtimist kui hajusjuhtimismeetodit kasutatakse võimsuse jagamiseks ja pinge stabiilsuse tagamiseks alalisvoolu nanovõrgus ilma täiendava andmesideta. Kui enamik olemasolevaid *droop*-juhtimismeetodeid keskendub iga üksiku aku väljundtunnusjoonte reguleerimisele, siis pakutud meetod muudab ainult ühte, võrguliidesmuunduri tunnusjoont, et kaudselt mõjutada akude laetuse taset. Meetod kasutab liigutatava käänupunktiga lõiguti lineaarset pingefunktsiooni, mida saab reguleerida vastavalt erinevatele stsenaariumidele. Väljapakutud juhtimismeetodi efektiivsust hinnati simulatsioonide abil, kasutades reaalseid mõõteandmeid katuse päikesepaneelidega elumajast. Tulemused näitavad, et pakutud meetod mitte ainult ei parenda aku kasutust, vaid suurendab ka taastuvenergia lokaalset tarbimist.